

# Tactile frequency discrimination is enhanced by circumventing neocortical adaptation

Simon Musall<sup>1-3,7</sup>, Wolfger von der Behrens<sup>2,4,7</sup>, Johannes M Mayrhofer<sup>2,3</sup>, Bruno Weber<sup>2,3</sup>, Fritjof Helmchen<sup>1,3</sup> & Florent Haiss<sup>2,5,6</sup>

Neocortical responses typically adapt to repeated sensory stimulation, improving sensitivity to stimulus changes, but possibly also imposing limitations on perception. For example, it is unclear whether information about stimulus frequency is perturbed by adaptation or encoded by precise response timing. We addressed this question in rat barrel cortex by comparing performance in behavioral tasks with either whisker stimulation, which causes frequency-dependent adaptation, or optical activation of cortically expressed channelrhodopsin-2, which elicits non-adapting neural responses. Circumventing adaptation by optical activation substantially improved cross-hemispheric discrimination of stimulus frequency. This improvement persisted when temporal precision of optically evoked spikes was reduced. We were able to replicate whisker-driven behavior only by applying adaptation rules mimicking sensory-evoked responses to optical stimuli. Conversely, in a change-detection task, animals performed better with whisker than optical stimulation. Our results directly demonstrate that sensory adaptation critically governs the perception of stimulus patterns, decreasing fidelity under steady-state conditions in favor of change detection.

How sensory information is transformed into a cognitive percept remains a major question in neuroscience. Numerous studies quantified how cortical activity relates to perception, either following sensory stimuli<sup>1-3</sup> or following direct cortical stimulation<sup>4-6</sup>. However, neural response properties are dynamic and modulated by contextual factors such as behavioral state, explorative movements or stimulus history<sup>7-9</sup>. A prominent and omnipresent feature in sensory systems is the rapid attenuation of responses with repeated stimulation<sup>10-12</sup>. Such adaptation can occur at different stages along the sensory pathway, including biophysical effects at sensory receptors<sup>13</sup> and adaptive discharge behavior of neurons in subcortical structures such as the brainstem<sup>14</sup> and thalamus<sup>11,15</sup>. Buildup of inhibition at various stages also contributes to adaptive response behavior<sup>16,17</sup>. However, adaptation is particularly strong in neocortex<sup>15,18-20</sup>, mainly as a result of short-term depression of thalamocortical synapses<sup>11,15,20</sup>. The main advantage of adaptation is believed to be increased coding efficiency by adjusting sensitivity of neural responses in accordance with prevailing conditions of the outside world<sup>21-23</sup>. Consistent with this notion, psychophysical studies have shown that presentation of an adapting stimulus sequence enhances discrimination of subtle differences between stimuli that are subsequently presented<sup>24,25</sup>. However, as neural responses are attenuated in relation to the amplitude of the adapting sequence<sup>21,26</sup>, the perceived intensity of subsequent stimuli is reduced accordingly<sup>27,28</sup>.

How does sensory adaptation affect perception when temporal information, such as stimulus frequency, needs to be extracted from

a uniform stimulus sequence? If frequency is defined by interpulse intervals of otherwise uniform stimuli (repetition frequency), increasing frequency might directly translate to increasing intensity because a sequence conveys more stimuli in a given amount of time<sup>29,30</sup>. However, adaptation also increases with shorter interpulse intervals<sup>11,23</sup>; high-frequency sequences therefore elicit stronger adaptation than lower frequencies. If frequency information is encoded by firing rates of cortical neurons<sup>29,31</sup>, adaptation might obstruct perception of frequency differences. More specifically, lower frequencies should be perceived more strongly because neural responses are less adapted than high-frequency sequences. Alternatively, repetition frequency might be conveyed by precise response timing regardless of changes in response amplitude<sup>32,33</sup>.

We addressed this question in the rat barrel cortex (BC), the whisker-related region in primary somatosensory cortex (S1) that is known to show strong and rapid adaptation specific for stimulus frequency and whisker identity<sup>1,11,20</sup>. For rats trained to perform in a two-alternative forced choice (2-AFC) task with bilateral single-whisker stimulation<sup>3</sup>, we found that discrimination performance of stimulus sequences with different repetition frequencies was explained by adaptation of neurons in BC. Optogenetic direct activation of BC neurons allowed us to circumvent sensory adaptation, which resulted in marked differences in animal behavior. Specifically, stimulus detection and discrimination of repetition frequency was strongly enhanced. Conversely, whisker-driven behavior could be replicated when optical stimulus trains were modified to mimic sensory-evoked adaptation, whereas reducing

<sup>1</sup>Brain Research Institute, University of Zurich, Zurich, Switzerland. <sup>2</sup>Institute of Pharmacology and Toxicology, University of Zurich, Zurich, Switzerland.

<sup>3</sup>Neuroscience Center Zurich, University of Zurich and ETH Zurich, Zurich, Switzerland. <sup>4</sup>Institute of Neuroinformatics, University of Zurich and ETH Zurich, Zurich, Switzerland. <sup>5</sup>Institute of Neuropathology, RWTH Aachen University, Aachen, Germany. <sup>6</sup>Department of Ophthalmology, RWTH Aachen University, Aachen, Germany.

<sup>7</sup>These authors contributed equally to this work. Correspondence should be addressed to S.M. (musall@hifo.uzh.ch).

Received 6 July; accepted 28 August; published online 21 September 2014; doi:10.1038/nn.3821

temporal precision had minor effects. In a change-detection task, with deviants embedded in the stimulus trains, animal performance was higher with whisker rather than optical stimulation. Taken together, our results indicate that adaptation enhances perception of salient stimuli at the cost of reducing fidelity under steady-state conditions.

## RESULTS

We first characterized sensory adaptation by performing extracellular recordings of S1 neurons in the C1-barrel column of awake rats (ten single units, 23 multi-units, 2 rats), in response to controlled deflections of the principal whisker. Stimulation with 1-s-long trains of pulsatile stimuli evoked a strong initial response followed by responses with progressively reduced response amplitude for the second and all subsequent pulses (Fig. 1a). The degree of adaptation was frequency dependent, showing stronger response attenuation with increasing frequency (Fig. 1b). To quantify this effect, we computed the adaptation index (AI) as the mean neural response to all stimuli except the first divided by the first stimulus response (spike counts within 25 ms after each pulse onset). The AI strongly decreased with frequency ( $AI_{5\text{Hz}} = 0.88 \pm 0.02$ ,  $AI_{10\text{Hz}} = 0.75 \pm 0.02$ ,  $AI_{20\text{Hz}} = 0.54 \pm 0.02$ ,  $AI_{30\text{Hz}} = 0.36 \pm 0.02$ ,  $AI_{40\text{Hz}} = 0.25 \pm 0.02$ , mean  $\pm$  s.e.m.,  $n = 33$  cells), consistent with previous findings on adaptation of BC neurons<sup>1,8,11</sup>. We were able to exclude strong modulation of adaptation during task engagement by performing additional recordings of S1 neurons in two rats that were actively engaged in the detection of 40-Hz sequences (Fig. 1c). Here, no significant difference to adaptation in passive animals was observed ( $AI_{\text{passive}} = 0.32 \pm 0.03$ , mean  $\pm$  s.e.m.,  $n = 33$ ;  $AI_{\text{active}} = 0.29 \pm 0.04$ ,  $n = 19$ ; unpaired  $t$  test,  $t_{50} = 0.59$ ,  $P = 0.5625$ ). Furthermore, we did not observe any systematic dependence of adaptation on cortical layer (Supplementary Fig. 1).

### Adaptation in S1 governs whisker-mediated behavior

To test the perceptual effect of adaptation, we trained three rats to perform a 2-AFC task for detection and discrimination of repetitive, pulsatile whisker stimulation (Supplementary Fig. 2a and Online Methods). In the detection task, the stimulus was applied to either the left or the right C1 whisker. A reward was given if the animal responded correctly by licking on the stimulus (target) side at one of two water spouts. Detection curves for individual pulses showed a sigmoidal shape with inflection points at half-optimal detection velocities ( $M_{50}$ ) ranging from 188 to 495  $^\circ\text{s}^{-1}$  (Fig. 1d). We then presented increasing numbers of pulses at  $M_{50}$  velocity with an inter-pulse interval of 25 ms (40 Hz). Although the single-pulse detection

rate was 17.9% above chance level, it only increased by an average of  $2.3 \pm 0.93\%$  for every extra pulse that was added to the sequence (Fig. 1e). Thus, detection performance with repeated stimulation was markedly lower than would be expected if every pulse had an equal perceptual weight<sup>1</sup>. However, when adaptation was considered by reducing the detection probability of subsequent pulses according to the observed  $AI_{40\text{Hz}}$  (Online Methods, Eq. (2)), the predicted curve matched the measured detection performance (Fig. 1e). These results imply that the animal's ability to detect uniform stimulus trains is indeed influenced by adaptation of cortical neurons.

Nonetheless, adaptation may still have little effect on discrimination of repetition frequency if such information would be encoded by spike timing. We therefore examined how well rats could perform bilateral discrimination of 1-s-long repetitive whisker stimulus trains presented at different repetition frequencies. For each rat, the  $M_{100}$  whisker velocity was chosen to match its respective optimal single-pulse detection performance (Fig. 1d). Again, rats had to lick on the side where a target stimulus was presented (randomly switching trial by trial between 20 Hz and 40 Hz as a target). Concurrent with the target on one side, another stimulus train with variable repetition frequency was presented on the opposite side as a distractor (1–35 Hz, always lower than the target repetition frequency; Supplementary Fig. 2a). Rats robustly detected target stimuli in the absence of any distractor ( $84.4 \pm 1.9$  and  $86.1 \pm 1.7\%$  for 20 and 40-Hz targets, respectively; mean  $\pm$  95% confidence interval (CI),  $n = 1,500$  trials), but a single pulse distractor was sufficient to significantly reduce behavioral performance to  $65.6 \pm 2.4\%$  (20-Hz target,  $\chi^2$  test,  $\chi^2(1) = 141.64$ ,  $P = 1.2 \times 10^{-32}$ ) and  $71.7 \pm 2.3\%$  (40 Hz,  $\chi^2$  test,  $\chi^2(1) = 93.32$ ,  $P = 4.4 \times 10^{-22}$ ). Discrimination performance further decreased with increasing distractor frequency, reaching levels that were not different from chance level for repetition frequencies close to the target. We presented 20-Hz sequences either as a target or distractor (against 40 Hz) and the rats could readily exchange target and distractor sequences depending on whether they were presented against a sequence of higher or lower repetition frequency (Fig. 1f).

The disproportionately large effect of a single pulse distractor can be explained by the rapid adaptation that follows the first pulse; the distractor would mask the simultaneously presented first pulse of the target sequence while subsequent pulses would already be adapted and insufficient for robust target identification. To test this hypothesis, we used a probabilistic model for stimulus detection and discrimination. Model performance was based on the integration of stimulus-evoked activity, derived from electrophysiological recordings of BC neurons

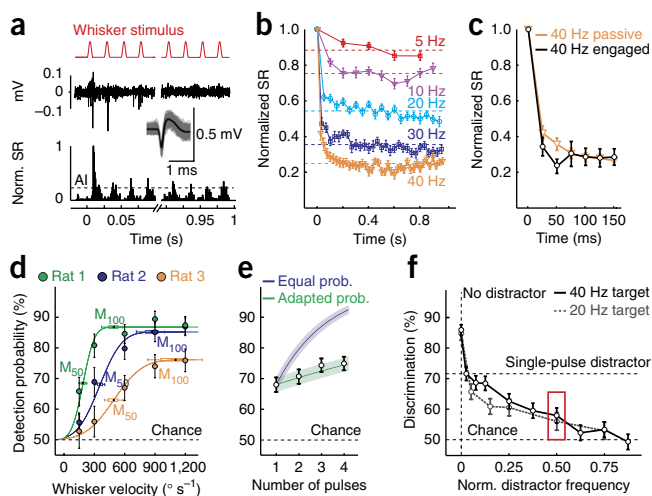


**Figure 1** Whisker-evoked cortical responses show frequency-dependent adaptation that affects performance in detection and discrimination tasks. (a) Extracellular recording in L2/3 BC following 40-Hz stimulation of the principal whisker. The initial and last four responses are shown. Inset, single-spike (gray) and mean (black) waveforms. Bottom, PSTH with spike rates (SR) normalized to the initial response. Dashed line shows the AI. (b) Normalized SR per whisker pulse at different frequencies for all recorded neurons. Dashed lines show AI levels. (c) Normalized SR in response to 40-Hz stimulation. Black circles show data from task-engaged animals and orange triangles from passive animals (as in b). (d) Velocity-response curves for detection of single-pulse whisker deflections. (e) Detection of stimulus trains with variable number of pulses at  $M_{50}$  velocity. Circles denote animal performance. Blue and green lines show either equal or adapted detection probability model, respectively. (f) Repetition frequency discrimination for 20- and 40-Hz target sequences, plotted against normalized distractor frequencies (distractor divided by target frequency). Red square highlights equal performance when 20 Hz was either target or distractor frequency. Error bars represent s.e.m. (b) and 95% CI (d-f) ( $n = 33$  cells).

**Figure 2** A model for repetition frequency discrimination based on neural response probabilities. **(a)** Illustration of our model for discrimination of a 40-Hz target versus a 5-Hz distractor sequence. For target and distractor, a single spike train was generated for each cell and summed into a population PSTH. PSTHs were normalized and convolved with an exponential decay kernel. Model responses were generated by subtracting the distractor from target PSTH and applying a threshold to the resulting differential PSTH. For each distractor, this approach was repeated for 1,500 trials. **(b)** Repetition frequency discrimination for 40-Hz target sequences (black), plotted against normalized distractor frequencies. Gray shading shows model discrimination performance. Error bars represent 95% CI. **(c)** Discrimination performance of two example cells. Cell 1 (blue trace and PSTH) showed low adaptation and high discrimination performance. This was reversed in cell 2 (green trace and PSTH). Error bars represent 95% CI. **(d)** Correlation between the  $AI_{40\text{ Hz}}$  of individual cells and their respective similarity index (SI) to optimal discrimination performance. Marked in green and blue are cells from **c**.

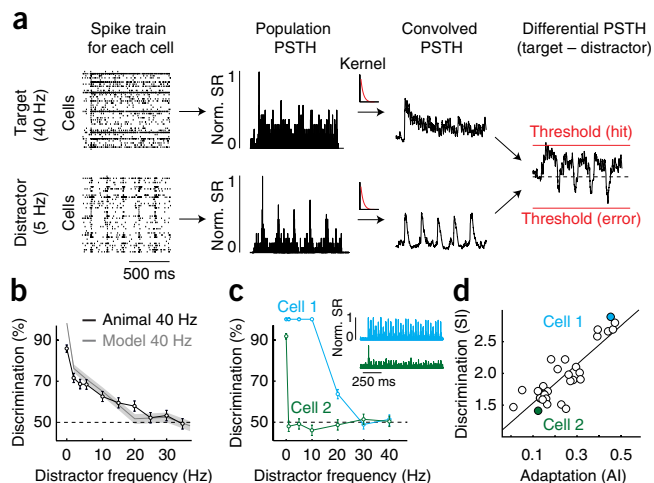


(**Fig. 2a**). More specifically, we constructed peristimulus time histograms (PSTHs) of the response probabilities of the population of recorded neurons for a target and distractor sequence. Both PSTHs were convolved with an exponential decay function and the distractor PSTH was subsequently subtracted from the target PSTH. A trial was counted as a hit when the peak spike count of the resulting differential PSTH exceeded the given threshold  $\alpha$  (**Supplementary Fig. 3** and **Online Methods**) and an error occurred if the differential PSTH fell below  $-\alpha$ . If the threshold was not crossed, a trial was counted as either a hit or error at 50% probability. The model could replicate the effect of single- and multi-pulse distractors on discrimination performance at varying repetition frequency and achieved performance levels that were highly comparable with trained animals (**Fig. 2b**). Notably, when PSTHs were based on single-cell responses, model discrimination performance varied between individual cells, but was strongly correlated with their degree of adaptation: neurons that adapted weakly displayed the strongest discrimination performance ( $r = 0.87$ ,  $P = 2.7 \times 10^{-10}$ ,  $n = 33$ ; **Fig. 2c,d**). Taken together, these results suggest that frequency-dependent adaptation not only determines the sensitivity of stimulus detection, but also markedly affects the animal's ability to discriminate sequences of different repetition frequency.

### Optogenetic stimulation improves behavioral performance

We next asked how sensory perception and task performance might be altered when adaptation is reduced. To circumvent sensory adaptation, we decided to stimulate BC neurons directly by expressing channel-rhodopsin-2 (ChR2) to optically drive spiking activity with blue light stimulation<sup>34</sup>. ChR2 was virally delivered into the C1 barrel columns in both hemispheres of the trained animals and induced robust ChR2 expression, spanning all layers (with reduced expression in layer 4) and extending  $2.1 \pm 0.3$  mm horizontally (mean  $\pm$  s.d.,  $n = 8$  injection sites in four trained rats; **Supplementary Fig. 4**). Short glass fiber tips (400- $\mu$ m diameter, connectorized to fiber optics and illumination system) were then implanted over the injection site (**Supplementary Fig. 2b** and **Online Methods**). Separate *in vivo* experiments in anesthetized rats confirmed that trains of blue light pulses induced high-fidelity spiking activity in individual neurons for frequencies up to 40 Hz (15 single units in 7 rats; **Fig. 3a** and **Supplementary Fig. 5**). This was also confirmed by additional recordings in an awake rat (**Supplementary Fig. 6**). As optical stimulation caused negligible adaptation of BC neurons ( $AI > 0.9$  for all frequencies), application of 1-ms light pulses

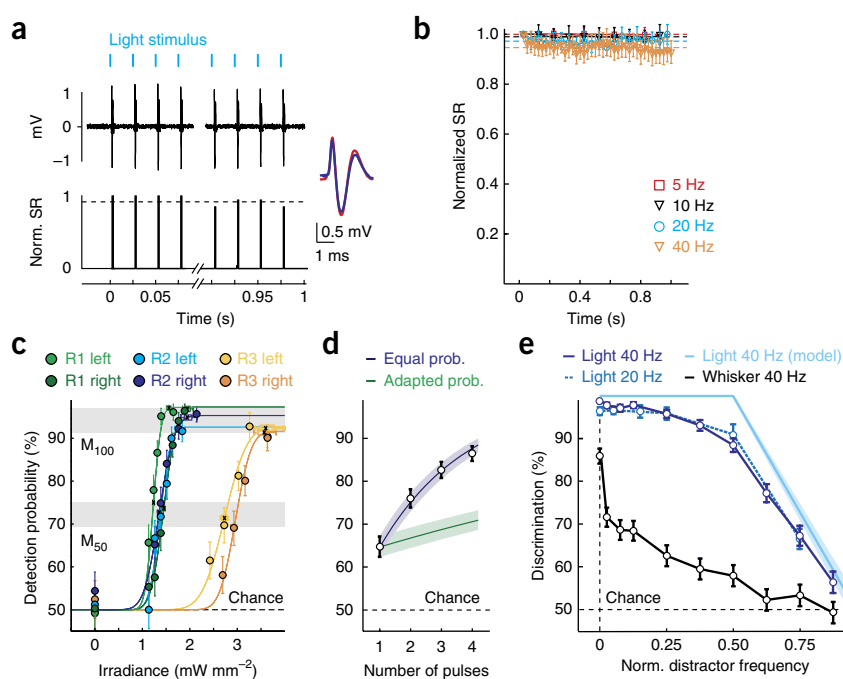


**Figure 3** Optogenetic stimulation induces adaptation-free responses that result in increased detection and discrimination performance. **(a)** Extracellular recording of BC neuron expressing ChR2. 1-ms blue light pulses induced spiking up to 40 Hz. Bottom, normalized PSTH over 50 trials. Inset, comparison of light-induced (red) and spontaneous (blue) waveforms. Dashed line denotes the AI. **(b)** Normalized SR per light pulse at different frequencies for all recorded neurons. Dashed lines show AI levels. **(c)** Irradiance-response curves for single light pulse detection. Gray bars mark minimal-to-maximal ranges for  $M_{50}$  and  $M_{100}$  values. **(d)** Detection of stimulus trains with variable number of light pulses. Data are presented as in **Figure 1e**. **(e)** Repetition frequency discrimination for 20- and 40-Hz target sequences using optical (dark/light blue) or whisker (black) stimulation. Performance is plotted against normalized distractor frequencies (distractor divided by target frequency). Light blue trace shows model performance. Error bars represent s.e.m. **(b)** and 95% CI **(c–e)** ( $n = 15$  cells).

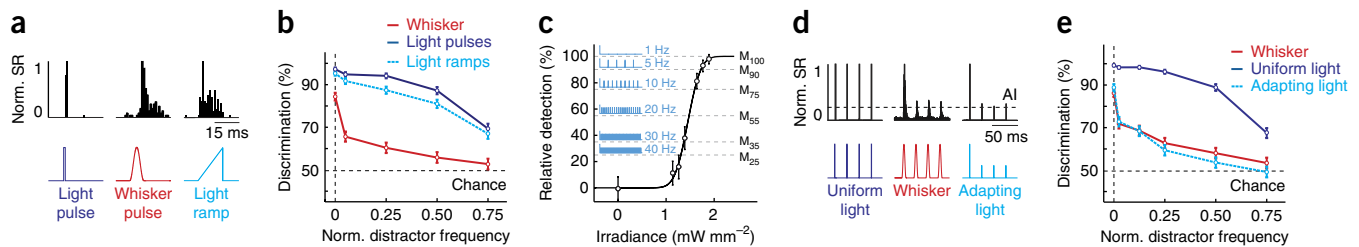


**Figure 4** Adapting light stimulation reproduces whisker-evoked repetition frequency discrimination performance. **(a)** Normalized PSTHs in response to different stimulus types (shown below traces). **(b)** Repetition frequency discrimination with light pulses (dark blue), whisker stimulation (red) and light ramps (light blue). **(c)** Example for construction of adapting light stimuli. On the basis of single light-pulse detection, we identified irradiance values that resulted in differential detection performance ( $M_{25}$ – $M_{100}$ ). Irradiance of the initial pulse was set to  $M_{100}$  amplitude, irradiance of subsequent pulses was set to match single-pulse detection performance and the adaptation index for the respective distractor frequency. **(d)** Normalized PSTHs in response to different 40-Hz stimulus sequences (shown below traces). **(e)** Discrimination performance with uniform light stimulation (dark blue), whisker stimulation (red) and adapting light stimulation (light blue). Error bars represent 95% CI. Performance is plotted against normalized distractor frequencies (distractor divided by target frequency, **b,e**).

instead of whisker stimuli allowed us to test behavioral performance under essentially adaptation-free conditions (**Fig. 3b**).

All three rats (as in **Fig. 1**) were able to detect light-induced target stimuli with high reliability after three to five sessions with light stimulation (~150–300 trials). To normalize perceived intensity of whisker and light stimuli, we measured psychometric curves with single light pulses of varying intensities for each hemisphere (**Fig. 3c**). Required light intensities for pulse detection were very low ( $M_{50\text{min}}$ ,  $1.22 \text{ mW mm}^{-2}$ ;  $M_{50\text{max}}$ ,  $2.92 \text{ mW mm}^{-2}$ ), suggesting that only neurons that were close (<0.35 mm) to the tip of the glass-fiber implant were activated by light (**Supplementary Fig. 4d,e**). We then repeated the target detection task with increasing numbers of light pulses using  $M_{50}$  light intensities. In contrast with whisker stimulation, detection rates with direct cortical stimulation were well explained by equal detection probability of individual pulses (**Fig. 3d**), consistent with earlier experiments using intracortical microstimulation<sup>35</sup>. This indicates that non-adaptive neural activation results in uniform perceptual weight of individual pulses in a sequence. Subsequently, we applied bilateral optical BC stimulation ( $M_{100}$  light intensities) using either 20 or 40 Hz as the target repetition frequency combined with various lower frequency distractors. Notably, discrimination performance based on light stimuli was significantly better than whisker stimulation (40-Hz targets, 25.8% root-mean-square error (RMSE), Kolmogorov-Smirnov test,  $D(10) = 0.7$ ,  $P = 0.0069$ ; **Fig. 3e**). Presentation of a single pulse distractor did not result in any significant decrease in discrimination performance (no distractor,  $97.3 \pm 0.8\%$  and  $98.9 \pm 0.5\%$ ; single pulse distractor,  $97.5 \pm 0.7\%$  and  $98.3 \pm 0.73\%$  for 20 and 40-Hz targets, respectively; mean  $\pm$  95% CI;  $\chi^2$  test,  $\chi^2(1)_{20\text{Hz}} = 0.2$ ,  $P_{20\text{Hz}} = 0.6547$ ;  $\chi^2(1)_{40\text{Hz}} = 1.99$ ,  $P_{40\text{Hz}} = 0.1583$ ), suggesting that the initial pulse in the target sequence did not carry disproportionately more perceptual weight than subsequent pulses. As a result of the previous perceptual calibration with whisker and optical stimulation, these behavioral differences cannot be explained by a general difference in perceived stimulus intensity (**Supplementary Fig. 7**). Based on the electrical recordings for different stimulation frequencies (**Fig. 3b**) we again modeled single-cell discrimination performance. Consistent with the experimental data, modeled discrimination performance was strongly enhanced compared with whisker stimulation over the range of distractor frequencies (**Figs. 1f** and **3e**).

#### Adapting optical stimulation mimics whisker stimulation

The marked behavioral differences between whisker and optical stimulation can be explained by the differential degree of adaptation. However, light stimuli not only induce non-adaptive firing, but also synchronous, millisecond-precise activation of cortical neurons.

Increased stimulus discrimination could therefore be a result of changes in adaptation or the sharp temporal profile of light-induced cortical activity. To address the latter possibility, we modified our light stimuli from 1-ms square-wave pulses to short 15-ms-long light ramps, which reduced time-locking of neuronal activation and resulted in a spread of stimulus response latencies comparable to whisker stimulation ( $\sigma_{\text{Whisker}} = 2.94 \pm 0.34 \text{ ms}$ ,  $\sigma_{\text{Ramp}} = 2.83 \pm 0.45 \text{ ms}$ , mean  $\pm$  s.e.m.,  $n = 15$ , unpaired  $t$  test,  $t_{46} = 0.18$ ,  $P = 0.8614$ ; **Fig. 4a** and **Supplementary Fig. 8**). Despite this reduction in temporal precision, light ramp stimulation barely reduced discrimination performance, which remained significantly different from whisker stimulation (RMSE 21.56%, Kolmogorov-Smirnov test,  $D(5) = 0.8$ ,  $P = 0.036$ ; **Fig. 4b**), indicating that temporal precision alone cannot account for the large difference to whisker stimulation.

To directly test whether sensory adaptation is the main cause of the behavioral differences, we adjusted our light stimuli to mimic sensory-evoked adapting responses. We reduced light irradiance during pulse sequences on the basis of the psychometric curves of individual animals so that, for each repetition frequency, the corresponding AI value for whisker stimulation was reached (**Fig. 4c**). For example, for 40-Hz stimulation, light irradiance of the initial pulse was set to optimal ( $M_{100}$ ) single pulse detection, whereas, for subsequent pulses, irradiance was reduced to 25% detection performance ( $M_{25}$ ) to match  $\text{AI}_{40\text{Hz}} = 0.25$  (**Fig. 4d** and **Online Methods**). Application of these adapting light stimuli in the behavioral procedure reduced the discrimination performance levels to values closely resembling the performance achieved with whisker stimulation (RMSE = 3.1%, Kolmogorov-Smirnov test,  $D(6) = 0.167$ ,  $P = 0.9996$ ; **Fig. 4e**). We conclude that detection, as well as discrimination, of repetitive sensory stimuli is largely governed by adaptation, whereas temporal precision has little effect on behavior.

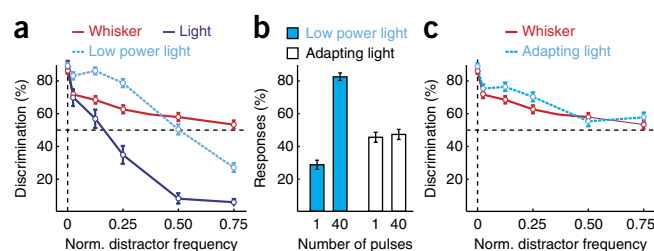
This conclusion is further supported by experiments in which 40-Hz whisker targets were paired with light distractors of lower repetition frequency (**Supplementary Fig. 2c**). When discriminating whisker from uniform light stimuli, rats were strongly biased toward light distractors with increasing repetition frequency. This bias was especially pronounced for distractor frequencies above 20 Hz, where animals almost exclusively chose light stimuli (**Fig. 5a**). To test if this bias could be reduced by decreasing light intensity, we also presented light distractors at  $M_{50}$  irradiance (**Fig. 5a**). Here, the rats performed better compared with whisker distractors for frequencies below 20 Hz, but remained biased toward light distractors at higher repetition frequencies. This asymmetric behavior with low light intensity was also observed when we tested the rats' stimulus preference by concomitantly presenting whisker and light

**Figure 5** Adapting light is comparable to whisker stimulation. (a) Discrimination performance using 40-Hz whisker targets versus whisker distractors (red) or uniform light distractors of either  $M_{100}$  (dark blue) or  $M_{50}$  (light blue) irradiance. (b) Animal stimulus preference with presentation of whisker and light stimuli of equal repetition frequency. Shown is the percentage of all trials in which rats responded toward light stimuli. Low power and adapting refer to the modality of light stimulus. (c) Discrimination performance using 40-Hz whisker targets versus whisker distractors (red) or adapting light distractors (light blue). Error bars represent 95% CI. Performance is plotted against normalized distractor frequencies (distractor divided by target frequency, a,c).

stimuli of equal repetition frequency (Fig. 5b). For single pulses, rats favored the whisker stimulus and rarely responded to the side that corresponded to the optical stimulus. However, in the case of 40-Hz trains, animals mostly preferred optical over whisker stimulation. Perception of uniform optical stimuli therefore differs from whisker stimulation depending on repetition frequency, even when light intensity is reduced. Conversely, rats showed no preference for either whisker or optical stimuli when adapting light stimulation was used. Furthermore, discrimination with 40-Hz whisker targets and adapting light distractors was not significantly different from pure whisker stimulation (RMSE = 5.54%, Kolmogorov-Smirnov test,  $D(6) = 0.4667$ ,  $P = 0.2851$ ; Fig. 5c).

#### Adaptation facilitates detection of deviant stimuli

Given the strong improvement in detection and discrimination behavior when circumventing adaptation, we also sought to address potential beneficial effects of adaptation. If the enhanced ability to discriminate subtle differences between stimuli after exposure to an adapting stimulus sequence is in fact a result of the adaptation of cortical neurons, detection of a deviant stimulus in a sequence should be easier with adapting responses to whisker stimulation than non-adapting light-evoked responses. We therefore added a single deviant stimulus to 20-Hz whisker stimulus trains. This protocol was verified by recording from BC neurons, with the amplitude of the 20-Hz sequence set according to the mean  $M_{50}$  detection performance across all tested rats ( $350^\circ \text{ s}^{-1}$ ) and the deviant amplitude set to mean



$M_{100}$  ( $850^\circ \text{ s}^{-1}$ ). Both stimuli induced robust neural responses in cortical neurons with a relative firing rate difference of  $\sim 50$  spikes per s (Fig. 6a). Response amplitude strongly adapted during the  $M_{50}$  pulse sequence, whereas the  $M_{100}$  deviant stimulus was less affected (Fig. 6b). Accordingly, the difference in neural response amplitude to uniform and deviant stimuli increased (non-adapted, 44.1%; adapted, 65.4%). This finding is consistent with a recent study showing that adaptation increases the threshold for neural responses to remain above the intensity of an adaptor sequence, whereas response amplitudes to stronger stimuli remain unchanged<sup>21</sup>.

To test whether this difference in neural responses would translate into improved perceptibility of deviant stimuli, we changed our behavioral task and bilaterally presented 2 20-Hz base sequences of either whisker or light stimuli at  $M_{50}$  amplitude to our trained rats. The target sequence (left or right) contained 1, 4 or 10 additional  $M_{100}$  deviant pulses after 1.5 s (Supplementary Fig. 2d). Rats were rewarded when they successfully identified the deviant-containing target sequence and omitted the uniform 20-Hz distractor sequence. In contrast to light stimulation in which detection of single deviants remained at chance levels ( $52.2 \pm 2.5\%$ , mean  $\pm$  95% CI, binomial test,  $P = 0.0933$ ), rats could detect the occurrence of a single whisker deviant ( $67.2 \pm 2.4\%$ , binomial test,  $P = 1.9 \times 10^{-41}$ ; Fig. 6c). The same result was observed in the model, where change detection was enhanced when base and deviant stimuli were adapted (non-adapted,  $53.1 \pm 2.5\%$ ; adapted,  $61.3 \pm 2.4\%$ ;  $\chi^2$  test,  $\chi^2(1) = 20.60$ ,  $P = 5.7 \times 10^{-6}$ ). For both whisker and light stimuli, performance further increased when additional deviant pulses were presented. Notably, there was no difference in behavioral performance for four and ten whisker deviants ( $81.7 \pm 2.0$  versus  $81.2 \pm 2.0$ ;  $\chi^2$  test,  $\chi^2(1) = 0.002$ ,  $P = 0.9643$ ), whereas performance with light stimulation continuously increased with deviant number. This dependency is to be expected when assuming that single deviants are more robustly detected as a result of their increased perceptual contrast against ambient stimuli, whereas repeated deviants are also subject to adaptation (Supplementary Fig. 9). For light stimulation, deviant detection

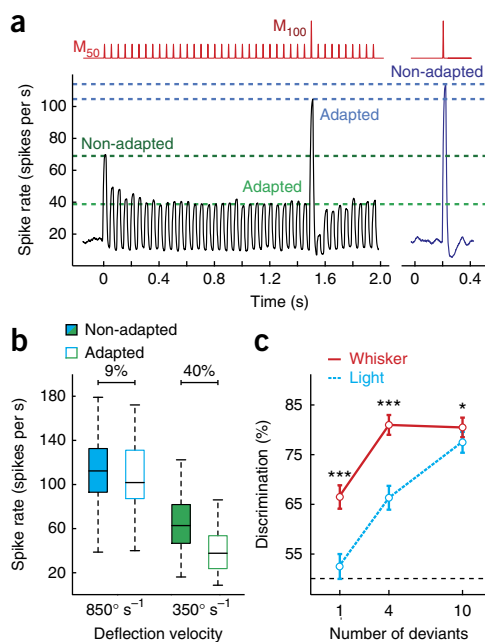


**Figure 6** Sensory adaptation facilitates deviant detection. (a) The black trace shows the neural response to a 20-Hz whisker stimulation sequence with a single deviant (top), averaged over all recordings. Response amplitude to subsequent pulses was decreased relative to the initial pulse (green lines), whereas deviant response amplitude remained close to non-adapted single-pulse responses (blue lines and dark blue trace). For display only, PSTHs were smoothed with a 25-ms moving average. (b) Firing rates over all recordings in response to non-adapted and adapted deviant ( $850^\circ \text{ s}^{-1}$ ) and base stimuli ( $350^\circ \text{ s}^{-1}$ ). The box shows the first and third quartiles, the inner line is the median. Box whiskers represent minimum and maximum values. (c) Deviant detection performance was better with whisker compared to light stimulation ( $\chi^2$  test, one deviant:  $\chi^2(1) = 61.35$ ,  $P = 4.8 \times 10^{-15}$ ; four deviants:  $\chi^2(1) = 84.98$ ,  $P = 3 \times 10^{-20}$ ; ten deviants:  $\chi^2(1) = 4.17$ ,  $P = 0.0411$ ). Error bars represent 95% CI.  $n = 33$  cells (a,b), 1,500 trials (c).

is directly related to the number of deviant presentations, analogous to detection of a pulse sequence (Fig. 3d). Consequently, the perceptual weight of ambient stimuli increases, obscuring identification of transient signal deviations.

## DISCUSSION

Our results indicate that animal behavior is shaped by sensory adaptation and provide a direct link between neural activity in the primary sensory cortex and stimulus perception. We found that sensory adaptation reduced the perceived intensity of uniform whisker deflection patterns, with the attenuation of neural responses being directly related to a reduced detection probability of repeated stimuli. Although reduced sensitivity to repeated stimulation has been demonstrated previously<sup>1</sup>, our results confirm that this is indeed well explained by adaptive response behavior of cortical neurons (Figs. 1e and 3d). Stimulus discrimination was also markedly affected by adaptation, being worse with whisker stimulation than non-adapting optical stimulation (Fig. 3e). This result might appear to contradict previous studies that showed a beneficial effect of adaptation to stimulus discrimination<sup>24,25,36</sup>. However, these earlier studies focused on the discrimination of instantaneous stimulus features (such as intensity or location) after presenting an adapting stimulus sequence, whereas we studied discrimination of simultaneously presented stimulus sequences that were adapting over time. In fact, our behavioral results, showing that adaptation enhances perception of change in a uniform stimulus sequence, are consistent with this earlier work.

The observed differences in behavioral performance indicate that the degree of adaptation has to be finely tuned to optimize cortical processing for solving a given task. Indeed, adaptation can dynamically change according to the behavioral state and different brain areas exhibit different degrees of adaptation<sup>7–9</sup>. Understanding the balance between change-perception and steady-state fidelity is essential for comprehending neocortical information flow and has clinical implications, as impaired adaptation has been associated with neuropsychiatric disorders, such as autism<sup>37,38</sup> and schizophrenia<sup>39</sup>. Combining optogenetic manipulation of neural response patterns and psychophysical assessment of the perceptual consequences is a promising path to achieve this goal.

Although several recent studies have used a combination of behavior and cortical stimulation to achieve a deeper understanding of the transfer from local-circuit activity to sensory perception<sup>5,6,40</sup>, the possibility to control neural adaptation had not been exploited up to now. With the presentation of light pulses in a 40-Hz sequence, we observed that the detection probability for each pulse remained constant and independent from the amount of presented pulses in a train (Fig. 3d). This corresponds to the observation that the number of stimulated sensory neurons can be traded off against the number of generated action potentials per neuron to produce the same perceptual intensity in a timeframe of up to 250 ms<sup>6</sup>. This activity has to be read out by higher order cortical areas, integrating the overall amount of action potentials in a given period of time. The fact that higher order networks, receiving S1 activity, appear to be able to optimally integrate all stimulus-evoked information<sup>41</sup> is surprising, especially in comparison with the strong modulation of perception by adaptation in S1 itself. Furthermore, it is important to note that intracortical synapses have also been shown to display adaptive response behavior<sup>42</sup>. Although it is probable that light stimulation drives a sufficient amount of neurons in S1 non-adaptively to provide a corresponding output to other areas, the implications of intracortical adaptation for signal integration in higher cortical areas remains unclear. A possible interpretation could be that synaptic transmission to higher order networks shows less depression<sup>43</sup> and integration of synaptic inputs operates over longer timescales as in

S1, which would also explain why we observed only minor behavioral effects when changing temporal precision of light-induced cortical activity. In contrast, neural synchrony in thalamus has been shown to be crucial to drive activity in cortex, suggesting a transformation from temporal to rate coding at the thalamocortical synapse<sup>36,44,45</sup>. A future experiment might involve expression of ChR2 in thalamus and subsequent activation of axonal arbors in cortex to test whether reduced temporal precision would result in corresponding changes in cortical firing and, eventually, animal behavior.

The finding that rats showed relatively low frequency discrimination performance is consistent with a recent study<sup>30</sup> demonstrating that rats perform poorly in detecting changes in frequency of an ongoing stimulus sequence. To understand the underlying mechanism, we used a theoretical model based on integration of firing rates in each hemisphere and detection of their relative difference (Fig. 2a). The fact that our psychometric data could be replicated by this simple approach (Fig. 2b) suggests that repetition frequency is mainly encoded by firing rates rather than by interspike intervals. Consequently, this rate code also explains how adaptation interferes with discrimination of stimulus sequences, as it reduces firing rates in a frequency-dependent manner<sup>11</sup>. In the context of texture discrimination, our findings support the hypothesis of texture coding by transient kinematic events, rather than frequency information<sup>30,46–49</sup>. When animals sweep their whiskers over a surface, they are deflected transiently as a result of discrete, high-velocity ‘slip-stick’ events<sup>46–49</sup>. The occurrence of such events is closely related to texture roughness, creating a detailed kinetic signature of different surfaces<sup>48</sup>. A contact sequence containing slip-stick events can be compared with pulse sequences containing velocity deviants, as we used (Fig. 6). The occurrence of tactile deviants evoked an increase in cortical activity that was close to non-adapted stimulus response amplitude, whereas the remaining sequence was strongly adapted. As a consequence, the contrast between uniform and deviant pulses was increased and deviant perceptibility was increased. This suggests that the main cue for texture discrimination might not be steady whisker vibration, but rather changes in firing rate that result from slip-stick events. In other words, firing rates of BC neurons would largely reflect the overall degree of stimulus diversity in a deflection pattern, rather than just the intensity of surface-induced whisker deflections. The encoding of such a diversity signal resulting from adaptation is supported by the notion that BC firing is increased with stimulus variance<sup>22</sup> and the enhanced perception of stimulus intensity when presented as irregular sequences in humans<sup>50</sup>.

The marked perceptual differences that we observed between sensory-evoked adapting and optically induced non-adapting S1 activity have implications for experimental approaches to induce synthetic sensory stimuli on the basis of neural stimulation. We and others have observed that artificial S1 stimulation can drive learned behavior on the basis of previous sensory stimulation<sup>4,5,40</sup>, suggesting that peripheral sensory input can be substituted by direct stimulation of cortical neurons. Moreover, animals that were trained to respond to S1 stimulation could readily transfer this behavior to whisker stimulation in a simple detection task<sup>5</sup>. In our 2-AFC setting, however, rats did require a certain amount of trials with light stimulation before reaching stable behavioral performance. In fact, it is not surprising that the perception of synthetic stimuli appeared to largely differ from peripheral stimulation (Figs. 3e, 4b and 5a). As we found, synthetic stimuli induced perceptions comparable to whisker stimulation when imposed with adapting time courses (Fig. 5c) up to the point where rats showed no preference for either optical or whisker stimulation when repetition frequency was equal (Fig. 5b). We therefore argue that synthetic stimulation approaches have

to consider adaptation rules to induce more naturalistic sensory perception. The emulation of adaptive response behavior could also serve as a basis for implementing effective cortical stimulation strategies for brain-machine interfaces or neuroprosthetics. Further optogenetic application could address the importance of different cell types and their functional connectivity, ultimately leading to optimized stimulation patterns that are naturally interpreted by neocortical circuits.

## METHODS

Methods and any associated references are available in the [online version of the paper](#).

*Note: Any Supplementary Information and Source Data files are available in the online version of the paper.*

## ACKNOWLEDGMENTS

We thank A. Saab, D. Margolis and B. Kampa for critically reading the manuscript, S. Weber for technical assistance, M. Durmaz for help with histological preparation, and Medartis AG for providing cortical screws. This work was supported by the EU-FP7 program (BRAIN-I-NETS project 243914 and BrainScales project 269921 to F. Haiss and F. Helmchen), the Swiss National Science Foundation (grant PP00B-110751/1 to B.W.), SystemsX.ch (project 2008/2011-Neurochoice to F. Helmchen and B.W.) and the Interdisciplinary Center for Clinical Research (IZKF Aachen) in the Faculty of Medicine at the RWTH Aachen University (to F. Haiss).

## AUTHOR CONTRIBUTIONS

S.M., W.v.d.B., J.M.M., F. Helmchen, B.W. and F. Haiss designed the study. S.M. and W.v.d.B. carried out experiments in the laboratory of B.W. J.M.M. and S.M. performed data analysis. F. Haiss and W.v.d.B. performed surgeries. F. Haiss, F. Helmchen, B.W. and S.M. wrote the paper.

## COMPETING FINANCIAL INTERESTS

The authors declare no competing financial interests.

Reprints and permissions information is available online at <http://www.nature.com/reprints/index.html>.

- Stüttgen, M.C. & Schwarz, C. Integration of vibrotactile signals for whisker-related perception in rats is governed by short time constants: comparison of neurometric and psychometric detection performance. *J. Neurosci.* **30**, 2060–2069 (2010).
- Adibi, M. & Arabzadeh, E. A Comparison of neuronal and behavioral detection and discrimination performances in rat whisker system. *J. Neurophysiol.* **105**, 356–365 (2011).
- Mayrhofer, J.M. *et al.* Novel two-alternative forced choice paradigm for bilateral vibrotactile whisker frequency discrimination in head-fixed mice and rats. *J. Neurophysiol.* **109**, 273–284 (2013).
- Romo, R., Hernández, A., Zainos, A. & Salinas, E. Somatosensory discrimination based on cortical microstimulation. *Nature* **392**, 387–390 (1998).
- Sachidhanandam, S., Sreenivasan, V., Kyriakatos, A., Kremer, Y. & Petersen, C.C.H. Membrane potential correlates of sensory perception in mouse barrel cortex. *Nat. Neurosci.* **16**, 1671–1677 (2013).
- Huber, D. *et al.* Sparse optical microstimulation in barrel cortex drives learned behaviour in freely moving mice. *Nature* **451**, 61–64 (2008).
- Fanselow, E.E. & Nicolelis, M.A.L. Behavioral modulation of tactile responses in the rat somatosensory system. *J. Neurosci.* **19**, 7603–7616 (1999).
- Castro-Alamancos, M.A. Absence of rapid sensory adaptation in neocortex during information processing states. *Neuron* **41**, 455–464 (2004).
- Hentschke, H., Haiss, F. & Schwarz, C. Central signals rapidly switch tactile processing in rat barrel cortex during whisker movements. *Cereb. Cortex* **16**, 1142–1156 (2006).
- Ulanovsky, N., Las, L., Farkas, D. & Nelken, I. Multiple time scales of adaptation in auditory cortex neurons. *J. Neurosci.* **24**, 10440–10453 (2004).
- Khatiri, V., Hartings, J.A. & Simons, D.J. Adaptation in thalamic barreloid and cortical barrel neurons to periodic whisker deflections varying in frequency and velocity. *J. Neurophysiol.* **92**, 3244–3254 (2004).
- Ohzawa, I., Sclar, G. & Freeman, R.D. Contrast gain control in the cat visual cortex. *Nature* **298**, 266–268 (1982).
- Fraser, G., Hartings, J.A. & Simons, D.J. Adaptation of trigeminal ganglion cells to periodic whisker deflections. *Somatosens. Mot. Res.* **23**, 111–118 (2006).
- Minnery, B.S. & Simons, D.J. Response properties of whisker-associated trigeminothalamic neurons in rat nucleus principalis. *J. Neurophysiol.* **89**, 40–56 (2003).
- Chung, S., Li, X. & Nelson, S.B. Short-term depression at thalamocortical synapses contributes to rapid adaptation of cortical sensory responses *in vivo*. *Neuron* **34**, 437–446 (2002).
- Hartings, J.A. & Simons, D.J. Inhibition suppresses transmission of tonic vibrissa-evoked activity in the rat ventrobasal thalamus. *J. Neurosci.* **20**, RC100 (2000).
- Hirata, A., Aguilar, J. & Castro-Alamancos, M.A. Influence of subcortical inhibition on barrel cortex receptive fields. *J. Neurophysiol.* **102**, 437–450 (2009).
- Hawken, M.J., Shapley, R.M. & Grosf, D.H. Temporal-frequency selectivity in monkey visual cortex. *Vis. Neurosci.* **13**, 477–492 (1996).
- Ulanovsky, N., Las, L. & Nelken, I. Processing of low-probability sounds by cortical neurons. *Nat. Neurosci.* **6**, 391–398 (2003).
- Katz, Y., Heiss, J.E. & Lampl, I. Cross-whisker adaptation of neurons in the rat barrel cortex. *J. Neurosci.* **26**, 13363–13372 (2006).
- Adibi, M., McDonald, J.S., Clifford, C.W.G. & Arabzadeh, E. Adaptation improves neural coding efficiency despite increasing correlations in variability. *J. Neurosci.* **33**, 2108–2120 (2013).
- Maravall, M., Petersen, R.S., Fairhall, A.L., Arabzadeh, E. & Diamond, M.E. Shifts in coding properties and maintenance of information transmission during adaptation in barrel cortex. *PLoS Biol.* **5**, e19 (2007).
- von der Behrens, W., Bäuerle, P., Kössl, M. & Gaese, B.H. Correlating stimulus-specific adaptation of cortical neurons and local field potentials in the awake rat. *J. Neurosci.* **29**, 13837–13849 (2009).
- Tannan, V., Simons, S., Dennis, R.G. & Tommerdahl, M. Effects of adaptation on the capacity to differentiate simultaneously delivered dual-site vibrotactile stimuli. *Brain Res.* **1186**, 164–170 (2007).
- Goble, A.K. & Hollins, M. Vibrotactile adaptation enhances amplitude discrimination. *J. Acoust. Soc. Am.* **93**, 418–424 (1993).
- Garcia-Lazaro, J.A., Ho, S.S.M., Nair, A. & Schnupp, J.W.H. Shifting and scaling adaptation to dynamic stimuli in somatosensory cortex. *Eur. J. Neurosci.* **26**, 2359–2368 (2007).
- Gescheider, G.A., Santoro, K.E., Makous, J.C. & Bolanowski, S.J. Vibrotactile forward masking: effects of the amplitude and duration of the masking stimulus. *J. Acoust. Soc. Am.* **98**, 3188–3194 (1995).
- Laskin, S.E. & Spencer, W.A. Cutaneous masking. I. Psychophysical observations on interactions of multipoint stimuli in man. *J. Neurophysiol.* **42**, 1048–1060 (1979).
- Gerjickov, T.V., Bergner, C.G., Stüttgen, M.C., Waiblinger, C. & Schwarz, C. Discrimination of vibrotactile stimuli in the rat whisker system: behavior and neurometrics. *Neuron* **65**, 530–540 (2010).
- Waiblinger, C., Brugger, D. & Schwarz, C. Vibrotactile discrimination in the rat whisker system is based on neuronal coding of instantaneous kinematic cues. *Cereb. Cortex* published online doi:10.1093/cercor/bht305 (29 October 2013).
- Luna, R., Hernández, A., Brody, C.D. & Romo, R. Neural codes for perceptual discrimination in primary somatosensory cortex. *Nat. Neurosci.* **8**, 1210–1219 (2005).
- Harvey, M.A., Saal, H.P., Dammann, J.F. III & Bensmaia, S.J. Multiplexing stimulus information through rate and temporal codes in primate somatosensory cortex. *PLoS Biol.* **11**, e1001558 (2013).
- Ewert, T.A.S., Vahle-Hinz, C. & Engel, A.K. High-frequency whisker vibration is encoded by phase-locked responses of neurons in the rat's barrel cortex. *J. Neurosci.* **28**, 5359–5368 (2008).
- Boyden, E.S., Zhang, F., Bamberg, E., Nagel, G. & Deisseroth, K. Millisecond-timescale, genetically targeted optical control of neural activity. *Nat. Neurosci.* **8**, 1263–1268 (2005).
- Butovas, S. & Schwarz, C. Detection psychophysics of intracortical microstimulation in rat primary somatosensory cortex. *Eur. J. Neurosci.* **25**, 2161–2169 (2007).
- Wang, Q., Webber, R.M. & Stanley, G.B. Thalamic synchrony and the adaptive gating of information flow to cortex. *Nat. Neurosci.* **13**, 1534–1541 (2010).
- Pellicano, E., Jeffery, L., Burr, D. & Rhodes, G. Abnormal adaptive face-coding mechanisms in children with autism spectrum disorder. *Curr. Biol.* **17**, 1508–1512 (2007).
- Tannan, V., Holden, J.K., Zhang, Z., Baranek, G.T. & Tommerdahl, M.A. Perceptual metrics of individuals with autism provide evidence for disinhibition. *Autism Res.* **1**, 223–230 (2008).
- Umbricht, D. & Krljes, S. Mismatch negativity in schizophrenia: a meta-analysis. *Schizophr. Res.* **76**, 1–23 (2005).
- O'Connor, D.H. *et al.* Neural coding during active somatosensation revealed using illusory touch. *Nat. Neurosci.* **16**, 958–965 (2013).
- Brunton, B.W., Botvinick, M.M. & Brody, C.D. Rats and humans can optimally accumulate evidence for decision-making. *Science* **340**, 95–98 (2013).
- Abbott, L.F., Varela, J.A., Sen, K. & Nelson, S.B. Synaptic depression and cortical gain control. *Science* **275**, 220–224 (1997).
- Gil, Z., Connors, B.W. & Amitai, Y. Efficacy of thalamocortical and intracortical synaptic connections: quanta, innervation, and reliability. *Neuron* **23**, 385–397 (1999).
- Bruno, R.M. & Sakmann, B. Cortex is driven by weak but synchronously active thalamocortical synapses. *Science* **312**, 1622–1627 (2006).
- Temereanca, S., Brown, E.N. & Simons, D.J. Rapid changes in thalamic firing synchrony during repetitive whisker stimulation. *J. Neurosci.* **28**, 11153–11164 (2008).
- Ritt, J.T., Andermann, M.L. & Moore, C.I. Embodied information processing: vibrissa mechanics and texture features shape micromotions in actively sensing rats. *Neuron* **57**, 599–613 (2008).
- Wolfe, J. *et al.* Texture coding in the rat whisker system: slip-stick versus differential resonance. *PLoS Biol.* **6**, e215 (2008).
- von Heimendahl, M., Itskov, P.M., Arabzadeh, E. & Diamond, M.E. Neuronal activity in rat barrel cortex underlying texture discrimination. *PLoS Biol.* **5**, e305 (2007).
- Jadhav, S.P., Wolfe, J. & Feldman, D.E. Sparse temporal coding of elementary tactile features during active whisker sensation. *Nat. Neurosci.* **12**, 792–800 (2009).
- Lak, A., Arabzadeh, E., Harris, J.A. & Diamond, M.E. Correlated physiological and perceptual effects of noise in a tactile stimulus. *Proc. Natl. Acad. Sci. USA* **107**, 7981–7986 (2010).

## ONLINE METHODS

**Animals and surgical procedures.** All experimental and surgical procedures were approved by the local veterinary authorities (Veterinary Office, Canton Zürich). They conformed to the guidelines of the Swiss Animal Protection Law, Veterinary Office, Canton Zurich (Act of Animal Protection 16 December 2005 and Animal Protection Ordinance 23 April 2008). Behavioral data with tactile and optogenetic stimulation were obtained from three female adult Sprague-Dawley rats (250–350 g). Additional electrophysiological data were obtained from two adult, female Sprague-Dawley rats under wakefulness and from seven female adult Sprague-Dawley rats under isoflurane anesthesia (see below). Rats were housed in groups of two with food *ad libitum* and were subjected to water deprivation for 5 d per week during behavioral testing. Body weight was monitored before each of the two daily testing sessions, during which water acted as reward. To ensure that animals' weight between training sessions remained above 90% of their initial weight, additional water was given if it dropped below this threshold. The animals were housed in groups of two under an inverted 12:12-h light-dark regime and trained during their active dark cycle.

In a first surgery, a head post was implanted as described previously<sup>3</sup>. In brief, animals were anesthetized with 2% isoflurane (vol/vol) in oxygen and nine titanium screws (Modus 1.5, 3-mm length, Medartis) were inserted into the skull, acting as anchors for the headcap. The headcap was formed by layers of transparent light-curing dental cement (Tetric EvoFlow, Ivoclar Vivadent) on top of a bonding layer (Gluma Comfort Bond, Heraeus Kulzer) that was applied to the cleaned skull. All animals were 12–15 weeks old on day of headpost implantation. In a second surgery, a viral construct that contained the ChR2 gene was injected into the C1 barrel in S1 under isoflurane anesthesia (1–2%). The head was fixed in a stereotaxic frame (David Kopf Instruments), the skull over the barrel cortex was thinned and a cortical response map was created using intrinsic optical imaging at 630-nm illumination<sup>51</sup>. Subsequently, a small craniotomy (~1 mm<sup>2</sup>) was made to allow injection of the viral construct AAV1.hSyn.hChR2-EFYP.WPRE.hGH (titer =  $5.7 \times 10^{-13}$  GC per ml, Penn Vector Core). For better diffusion in tissue, 1  $\mu$ l of 30% Mannitol (wt/vol) was added to 1.5- $\mu$ l aliquots of virus solution. To prevent dimpling of the brain, the dura was incised at the injection site. For each hemisphere, a total amount of 1  $\mu$ l was injected using a microinjection pump (WPI) and pulled glass pipettes. Injection depth was 500  $\mu$ m and the flow rate 50 nl min<sup>-1</sup>. After virus injection, a multimode glass fiber (length ~6 mm, diameter = 400  $\mu$ m, NA = 0.48, Thorlabs), glued into a short stainless steel ferrule (length ~5 mm) was positioned above the injected barrel. The ferrule was then fixed to the headcap using light-curing dental cement. After surgery, animals were provided with analgesics (110 mg per kg of body weight, Novaminsulfon; Sintetica) and antibiotics (100 mg per kg, Ceftriaxon, Rocephin, Roche Pharma). For each animal, we waited at least 4 weeks for expression of ChR2 before starting behavioral testing with blue light stimulation.

**Histology and estimate of light transmission in cortex.** The mean extent of ChR2 expression for all injections was  $2.1 \pm 0.3$  mm (mean  $\pm$  s.d.) and highly consistent across all behaving animals and injection sites. Expression of ChR2 was observed over all cortical layers, but appeared to be strongly reduced in layer 4 of the affected barrels. To estimate the size of the illuminated area in cortical tissue, we used a theoretical model based on measurement of light transmission through brain slices (Supplementary Fig. 4d)<sup>52</sup>. To generate model estimates, we used the brain tissue light transmission calculator (<http://www.stanford.edu/group/dlab/optogenetics/calc>), provided by the Deisseroth laboratory. The lowest required intensity for robust single pulse detection was  $1.6$  mW mm<sup>-2</sup> at the brain surface. At a distance of 0.18 mm, light irradiance was  $0.5$  mW mm<sup>-2</sup>, which, to the best of our knowledge, is the lowest intensity that has been shown to induce spiking in awake animals<sup>53</sup>. Assuming that light might also affect neurons slightly below this value, we therefore estimate that light stimulation should only drive neural activity in a distance of about ~0.35 mm from the fiber tip (until irradiance was below half of  $0.5$  mW mm<sup>-2</sup>). Also, when applying the simplified assumption that light spreads equally in all directions from the fiber tip, it is also possible that adjacent barrels were affected by light stimulation. In addition, we observed some changes in local axonal morphology, potentially as a result of long-term expression of ChR2 (Supplementary Fig. 4f)<sup>54</sup>.

**Behavioral setup and procedures.** Three female adult rats were trained to perform in a 2-AFC procedure for detection and discrimination of whisker stimuli.

The behavioral setup has been described in detail previously<sup>3</sup>. In brief, animals were placed in a head fixation box and the C1-whiskers were stimulated with a set of piezo bending actuators (Piezo Systems). Whisker stimuli consisted of individual or uniform sequences of prototype pulses (single-period 120-Hz cosine wave). Whisker deflection velocity was changed by modifying prototype peak amplitude (maximal deflection amplitude = 300  $\mu$ m), whereas frequency was changed by varying interpulse time intervals (Supplementary Fig. 10). Animals performed three different tasks: detection of single stimuli or stimulus trains, discrimination of stimulus trains at different repetition frequency and detection of deviant pulses of higher deflection velocity. During stimulus detection, stimuli were presented to either the left or the right C1 whisker and animals received a water reward when correctly responding to the respective stimulus side by touching one of two water spouts (positioned to the left and right in front of the animals head) with their tongue. Initially, head-fixed animals had to detect single pulsatile stimuli of differing velocities. The resulting detection performance of every animal was then used to adjust whisker deflection velocities during subsequent behavioral testing (see below and Fig. 1d). To test detection performance with increasing pulse counts, deflection velocities were adjusted to M<sub>50</sub> detection performance and short trains of pulsatile stimuli of differing lengths (1–4 pulses with an interpulse interval of 25 ms) were presented to the animal. During repetition frequency discrimination, animals had to compare pairs of vibrotactile stimuli that were presented simultaneously at both whiskers. Deflection velocities were set to M<sub>100</sub> detection performance. High repetition frequency stimuli (20, 40 Hz) were always considered as the target, which had to be chosen over a distractor stimulus of lower repetition frequency (1, 3, 5, 10, 15, 20, 25, 30, 35 Hz). Trials of different target and distractor repetition frequency were randomly intermixed in each session. 20-Hz sequences could occur as either target or distractor stimuli, thereby ensuring that animals had to rely on repetition frequency to discriminate sequences instead of identifying a constant target percept (Supplementary Fig. 10b). For deviant detection, a 2-s-long, vibrotactile stimulus at 20 Hz and M<sub>50</sub> deflection velocity was presented at both whiskers. After 1.5 s, a deviant at M<sub>100</sub> deflection velocity was embedded in the target stimulus. The deviant sequence was 1, 4 or 10 pulses long and animal's response after deviant occurrence was measured to compute deviant detection performance.

Trial structure was as follows. After trial start, stimuli were presented after 2.5 s with a temporal jitter of up to 30% to avoid animal's prediction of stimulus occurrence. A no-lick period of 1 s before stimulus onset was used. Licks that occurred in this period resulted in a shift of the stimulus onset by 1 s (Supplementary Fig. 10c). Stimulus duration was 1 s for stimulus detection and discrimination and 2 s for deviant detection. Stimuli were presented to either the left or the right C1 whisker and animals received a water reward when correctly responding to the stimulus side by licking the respective water spout. The decision period at which the animal's response was measured was 2 s after stimulus onset or occurrence of the deviant in case of deviant detection. Two additional rats were trained on detection of 40-Hz sequences at M<sub>100</sub> velocity to obtain electrophysiological recordings of BC neurons in task-engaged animals.

**Optogenetic stimulation.** For light stimulation, we connected the glass fiber implants with ~1-m-long glass fibers (diameter = 1,000  $\mu$ m, NA = 0.48, Thorlabs) that were attached to high-power LED light sources ( $\lambda$  = 470 nm, Nichia). Light stimuli consisted of pulse trains with equal frequencies as during whisker stimulation. Each pulse consisted of a 1-ms-long square wave. Again, single light pulse detection performance was used to assess the required light intensities for subsequent behavioral testing (intensity was measured for each hemisphere individually). In each animal, we tested responsiveness to light pulses repeatedly over the course of behavioral testing and adjusted light intensity accordingly (Supplementary Fig. 11). This was usually done between different behavioral procedures. For rat 1, the second test was performed earlier after we noticed an imbalance in stimulus perception between left and right hemisphere (Supplementary Fig. 11a). Behavioral procedure for stimulus detection, discrimination and deviant detection were the same for both whisker and light stimulation. To reduce temporal precision of neural excitation, 1-ms pulses were subsequently modified to 15-ms light ramps of monotonically increasing intensity (Fig. 4a). Here, stimulus discrimination was tested only with frequencies up to 20 Hz because we observed unreliable response behavior of stimulated neurons with 40-Hz light ramp sequences (Supplementary Fig. 8). This change in reliability is most likely a result of the 15-ms duration of light ramps, reducing the duration

of the break between two ramps to 10 ms (instead of 24 ms with 1-ms pulses), which is too short to ensure sustained ChR2 stimulation<sup>34</sup>. To recover adaptive neural behavior during light stimulation, light amplitude of non-initial pulses was modified according to adaptation indices derived from electrophysiological recordings. The initial pulse in a sequence was set to  $M_{100}$  amplitude, following pulses were reduced depending on stimulus frequency and single pulse detection performance (for more details, see below). For all procedures, we used 500 trials per animal and condition, resulting in 1,500 trials in total. Only when combining whisker targets with uniform light distractors (Fig. 5a) were less trials acquired at higher distractor frequencies, resulting from the strongly biased animal behavior (at least 150–200 trials per animal). For an overview of the complete training schedule for different behavioral procedures, see **Supplementary Figure 12**. In the case of stimulus discrimination with low light power (500 trials per data point; **Supplementary Fig. 7**), only one animal was tested (rat 3).

To ensure that animals would not be able to use visual cues from light stimulation, fibers and connectors were shielded with black rubber tubing. In addition, a blue LED was positioned ~10 cm above the animals head. This masking LED produced light flashes (irradiance = 150 mW mm<sup>-2</sup>) of equal length as every light pulse presented on the brain surface, thereby preventing the animal from associating potential visual cues with target or distractor side. To keep conditions constant over all behavioral sessions, the masking LED was also active during whisker stimulation (producing 1-ms light pulses for every whisker deflection). Whisker movements during optogenetic stimulation (**Supplementary Fig. 13**) were monitored with a laser curtain and a linear CCD array (3.5- $\mu$ m resolution at 2.5-kHz sampling rate, RX 03, Metralight). To ensure robust tracking of whisker motions, a light polyimide tube (weight = 0.7 mg, diameter = 250  $\mu$ m) was put on the C1 whisker. All components of the setup were controlled and monitored with millisecond temporal precision by a custom-written program (LabVIEW 2010, National Instruments) running on personal computers using multifunctional data acquisition cards (PCI-6259, National Instruments).

**Electrophysiological recordings.** For electrophysiological recordings in awake animals two adult, female Sprague-Dawley rats were chronically implanted with single shank, 16-contact electrode arrays with 100- $\mu$ m contact spacing (NeuroNexus). Surgical procedures were the same as for implantation of glass fibers (see above). We implanted two probes in rat 1 (one on each hemisphere) and a single probe in rat 2, resulting in 48 recording sites in total. Ten sites were removed from the analysis as they showed no visible spiking activity; from the remaining, we recorded 10 single-units and 23 multi-unit clusters over all cortical layers. Adaptation of individual recording sites and layers are shown in **Supplementary Figure 1**. Recordings were made with a commercially available system (Multi Channel Systems MCS), consisting of two 8-channel pre-amplifiers (2 $\times$  gain), a 64-channel amplifier (600 $\times$  gain) and a 64-channel PCI-bus data acquisition card. Data were digitized with a bandwidth of 0.1 Hz to 15 kHz at 32 kHz and 12 bit. For stimulation, we used piezo bending actuators (Piezo Systems) that were driven by a 3-channel piezo controller (Thorlabs). Movement of the stimulator was calibrated with a laser displacement sensor (Micro-Epsilon) and strain gauge sensors mounted directly on the piezo element. Single whiskers were plugged into a glass capillary that was glued on the element. The distance between capillary tip and whisker base was ~5 mm and we always stimulated the whisker that corresponded to the recorded barrel (either C1 or D1). Each trial consisted of a 1-s baseline and 1–2-s stimulus presentation. Intertrial duration was 2 s. Different stimuli were presented in randomized order. We recorded neural responses to three sets of stimuli: First, single whisker pulses at differing velocities (150, 300, 600, 900 and 1,200 ° s<sup>-1</sup>). Second, 1-s-long pulse trains with a whisker velocity of 850 ° s<sup>-1</sup> and different frequencies (1, 5, 10, 20, 30 and 40 Hz). Third, 2-s-long pulse trains with a velocity of 350 ° s<sup>-1</sup> and repetition frequency of 20 Hz with and without deviant pulses (1, 4 or 10 pulses with a velocity of 850 ° s<sup>-1</sup>) after 1.5 s. In the same set, we also presented single pulses with a velocity of 350 or 850 ° s<sup>-1</sup>. To acquire a sufficiently high amount of trials in response to all presented stimuli, different stimulus sets were presented in separate recording sessions. In each session, animals were recorded for a total duration of up to 40 min. All three recording sessions were always performed within 24 h. Visual data inspection showed no observable difference in recording quality or spontaneous activity of neurons. For recordings in task-engaged animals, two trained, female Sprague-Dawley rats were implanted with 16-contact electrode arrays in the left hemisphere. Surgical procedures were the same as described above. Animals

were trained to detect 40-Hz whisker stimulus sequences, applied to the principal whisker and we recorded responses from 19 recording sites across all cortical layers (**Supplementary Fig. 2c**).

To record neural responses to light stimulation, we acquired electrophysiological data under isoflurane anesthesia from seven female adult Sprague-Dawley rats. Animal temperature was monitored with a rectal temperature probe and maintained at 37 °C by a feedback-controlled heating pad (Harvard Apparatus). The head was fixed in a stereotaxic frame (David Kopf Instruments). After exposing the skull, the bone over the left barrel cortex was thinned and the corresponding whisker representation was identified using intrinsic optical imaging. A small (~2 mm<sup>2</sup>) craniotomy was made and the dura was incised at the point of penetration. Lastly, a small acrylic dam was built around the skull opening and filled with saline. To record neural activity from individual neurons, pulled borosilicate glass pipettes with an impedance of 7–10 M were used. Pipettes were filled with 0.9% NaCl (wt/vol) solution and connected to a silver wire that was used for recording. To identify ChR2-expressing neurons, we used a light pulse at low repetition rate (1 ms, 0.5 Hz) while moving through cortex and only recorded cells that showed consistent responses to light stimulation. This was the case for roughly 75% of all encountered neurons. We recorded well-isolated single units ( $n = 15$ ) and performed additional control recordings to ensure that glass pipette recordings were not contaminated by any potential light induced artifacts<sup>55</sup> (data not shown). For illumination, we used ~1-m-long glass fibers (diameter = 400  $\mu$ m) that were connected to a blue diode laser ( $\lambda = 473$  nm, Micron-Laserage) and positioned directly above the recording site. For each recorded neuron we presented 1-s-long stimulus trains (peak irradiance = 100 mW mm<sup>-2</sup>) of differing frequencies (1, 5, 10, 20 and 40 Hz) and pulse durations (either 1-ms-long square-wave pulses or continuously increasing 15-ms-long ramps). Different frequencies and single pulse profiles were presented in the same recording session in pseudo-randomized order. Electrophysiological data were 1,000-fold amplified and digitized at 32 kHz and 16 bit with a bandwidth of 1 Hz to 5 kHz, using a commercially available USB recording system (Multi Channel Systems). The same system was also used for recording neural responses to light stimulation in one female Sprague-Dawley rat that was awake, but not engaged in a behavioral task. Here, a 400- $\mu$ m diameter glass fiber was connected to a 16-contact electrode array (as described above) using dental cement. The array was implanted in BC of the left hemisphere and we recorded neural responses from 12 recording sites in response to optical stimulation at 20 and 40 Hz (**Supplementary Fig. 6**). Optical stimuli were delivered as described for behaving animals and peak irradiance was set to 100 mW mm<sup>-2</sup>.

**Behavioral data analysis.** All data analysis procedures were implemented using MATLAB (2010b, Mathworks). The data set consisted of behavioral recordings from three rats in three conditions (stimulus detection, repetition frequency discrimination and deviant detection) with whisker, light or combined stimulation. A trial was counted as correct (hit) when the animal's initial response was on the target side or as a false (error) in the opposing case. A no-lick response in the 2-s time window after the start of the decision period was classified as a missed trial. Performance was computed as number of hits/(number of hits + number of errors). To test for significant differences between behavioral conditions, we used a Pearson's  $\chi^2$  test. To test if behavioral performance differed from chance we used a two-sided binomial test. To avoid any multiple comparison bias, we additionally applied Bonferroni correction for the required  $P$  value to reach significance. Statistical comparison of discrimination curves was done by using a two-sample Kolmogorov-Smirnov test. The RMSE was computed as the root-mean-square of the difference between two curves. To analyze psychometric single-pulse detection curves, we used a Matlab toolbox for psychophysical data analysis (version 2.5.6; <http://bootstrap-software.org/psignifit/>). To adjust fit parameters and obtain statistical significance, the toolbox implements the maximum-likelihood method described previously<sup>56</sup>. We fitted a cumulative Gauss function to detection performance of individual animals and computed the turning point and asymptote (corresponding to  $M_{50}$  and  $M_{100}$ , respectively). In case of single light pulse stimulation, we additionally computed different values on the curve that corresponded to AIs of different frequencies (40 Hz –  $M_{25}$ , 30 Hz –  $M_{35}$ , 20 Hz –  $M_{55}$ , 10 Hz –  $M_{75}$ , 5 Hz –  $M_{90}$ ). The resulting light intensities of each individual hemisphere were later used to determine the degree of attenuation of repeated pulses in 'adapting light' stimulus sequences (**Fig. 4c**).

For detection of stimulus sequences at varying pulse counts, the estimation of equal detection probability was based on the assumption of combinatorial probability of detecting at least one pulse in a sequence of  $n$  pulses

$$P_{\text{Sequence}} = 1 - (1 - P_{\text{Pulse}})^n \quad (1)$$

To explain reduced detection probability of subsequent pulses by attenuation of neural response amplitude, the AI for 40 Hz was added to the second and further pulse detection probability.

$$P_{\text{Adapted Sequence}} = 1 - (1 - P_{\text{Pulse}}) * (1 - P_{\text{Pulse}} * AI_{40 \text{ Hz}})^{n-1} \quad (2)$$

To apply both approaches to the 2AFC configuration, the minimum detection probability  $P_{\text{Chance}}$  was fixed at 50%. To correct for chance detection probability,  $P_{\text{Pulse}}$  was therefore computed as

$$P_{\text{cPulse}} = (P_{\text{Pulse}} - P_{\text{Chance}}) / (1 - P_{\text{Chance}}) \quad (3)$$

Finally, to maintain comparability to the measured behavioral data, chance performance was again added to  $P_{\text{cSequence}}$ :

$$P_{\text{cSequence}} = P_{\text{cSequence}} * (1 - P_{\text{Chance}}) + P_{\text{Chance}} \quad (4)$$

To estimate animal reaction times, we also computed median response times during whisker and light stimulation. Response time was calculated as the time difference between stimulus onset and the first lick response that was detected. We analyzed response times for successful detection of 40-Hz stimulus trains (7,000 trials per animal, 21,000 trials in total) for each whisker and light stimulation (**Supplementary Fig. 14**). Significance between reaction times with whisker and light stimulation was computed with a Wilcoxon rank-sum test for equal medians.

**Electrophysiological data analysis.** Raw-data was high-pass filtered at 600 Hz and thresholded to identify spike occurrence. For multi-unit activity, a threshold of 4 s.d. units was used. For single-unit activity, the threshold was set to 15 SDUs. Resulting spike times were then downsampled to 1 kHz. In all subsequent analysis, we only used one individual session per stimulation procedure and recording site. In awake recordings, trials that contained transients resulting from animal movement could be reliably identified by scanning for instantaneous occurrence of spiking in all 16 recording channels. Trials that met this criterion were removed from the analysis (~12% of all trials, remaining trial count per stimulus type and session varied from 71 to 103). In case of task-engaged recordings, we only analyzed trials in which animals produced a behavioral response (hit or error). In this case, we also analyzed only the first 175 ms after stimulus-onset to avoid data contamination by movement artifacts that were due to licking responses of the animal. We used the Glass's  $\Delta$  for single-pulse spike probabilities as a measure for the signal-to-noise-ratio (SNR) of each recording. Glass's  $\Delta$  was computed as

$$D = (mean_{\text{Signal}} - mean_{\text{Baseline}}) / SD_{\text{Baseline}} \quad (5)$$

where  $mean_{\text{Signal}}$  is the mean neural response within 25 ms of the onset of the first pulse in a stimulus sequence and  $mean_{\text{Baseline}}$  the mean spontaneous activity 25 ms before stimulus onset.  $SD_{\text{Baseline}}$  is the respective s.d. To extract firing probabilities, we computed the PSTH for every recording, repetition frequency and stimulus type (bin size = 1 ms).

For AIs, we computed the mean firing within 25 ms of each whisker or light pulse for stimulus sequences of varying repetition frequency. Subsequently, we subtracted the mean baseline activity (500 ms before stimulus onset) and normalized all values relative to the initial pulse response amplitude (**Fig. 1b**). AIs were defined as the mean response strength of all pulses except the first one in each stimulus sequence. To ensure that AIs were not spuriously high due to low SNR, only recordings with a Glass's  $\Delta > 0.5$  were used for this analysis (33 of 38 units).

To test for differences in the spread of stimulus response latencies between whisker and 15-ms light ramp stimuli, we fitted each PSTH for single stimulus presentation with a Gauss distribution and used the s.d.  $\sigma$  as a measure of the distribution width. Significance was obtained using a two-sided, unpaired  $t$  test.

During deviant presentation, we computed the mean response strength within 25 ms of presentation of single pulses at mean  $M_{50}$  ( $350^\circ \text{ s}^{-1}$ ) and  $M_{100}$  ( $850^\circ \text{ s}^{-1}$ ) amplitude (non-adapted response). For adapted responses, we computed the mean response strength to either an  $M_{100}$  deviant or a standard  $M_{50}$  pulse in 20-Hz sequences at  $M_{50}$  amplitude after 1.5 s. To test for significant differences between adapted and non-adapted responses, we used a two-sided, paired  $t$  test. Before  $t$  testing, we performed a Lilliefors test on each condition to confirm they followed a normal distribution ( $P > 0.05$  for all tested cases).

**Modeling of behavioral performance.** Based on a previous study<sup>1</sup>, we constructed a theoretical model to relate behavioral performance to neural activation patterns during different conditions. For each cell ( $n = 33$ ), we used its respective PSTH to construct a single Monte-Carlo sampled spike train. Spike trains of all cells, were then summed together to compute a population PSTH in response to a single stimulus presentation. To include temporal integration, the population PSTH was convolved with an exponential decay function of the form  $\exp(-t/\tau)$  (normalized to have an integral of 1, where  $t$  is time in milliseconds). To approximate membrane time constants of pyramidal cells in adult animals, the time constant  $\tau$  was set to 20 ms (ref. 57). The same procedure was repeated to compute two convolved population PSTHs, mimicking the two respective hemispheres in a 2-AFC condition. As in our behavioral procedure, one PSTH was computed using a higher repetition frequency as a target, the other with lower repetition frequency as a distractor. Subsequently, the distractor PSTH was subtracted from the target PSTH. If the peak spike count of the resulting differential PSTH exceeded a threshold  $\alpha$ , the trial was counted as a hit. Conversely, if spike counts went below a negative threshold  $-\alpha$ , the model produced an error. The first threshold crossing after stimulus onset was always used to determine model behavior. In trials where the threshold was not crossed model performance was fixed at chance levels and therefore trials were either counted as hit or error with 50% probability. In each condition, the above procedure was repeated for 1,500 trials. An illustration of the model is given in **Figure 2a**. The same approach was also used for adapting and non-adapting single pulse discrimination. Here, recordings of 20-Hz base sequences with and without occurrence of a single deviant were used to obtain target and distractor PSTHs and perform adapting pulse discrimination. Only threshold crossings after deviant occurrence were taken into account. Non-adapting pulse discrimination was achieved by using neural responses to single pulses of deviant (target) and base (distractor) amplitude.

To determine the detection threshold  $\alpha$ , we tuned the model by detecting single whisker deflections of varying amplitude (150, 300, 600, 900 and  $1,200^\circ \text{ s}^{-1}$ ) against stimulus-free spontaneous activity. We tested different thresholds between 0.05 and 1 with a step size of 0.01 and each resulting model was compared to animal's mean single pulse detection performance. Animal performance was normalized by dividing with its maximum, thus allowing the model to obtain optimal detection performance while still resembling the same psychophysical dynamics. Similarity index  $S$  between animal and model performance was computed as

$$S = \log(1/RMSE) \quad (6)$$

where RMSE is the root-mean-squared error between real and modeled detection performance. The highest similarity was achieved by using a threshold of  $\alpha = 0.64$ . As shown in **Supplementary Figure 3b**, the model exceeded animal's detection performance, and both single pulse detection curves were well described by a cumulative Gaussian function and had almost identical inflection points. This indicates that our theoretical approach was fit to resemble animal behavior in a 2AFC condition while achieving strong signal detection performance. The same threshold was used during all behavioral conditions, i.e. repetition frequency discrimination and deviant detection. In addition, we used the same approach as described above but created spike traces solely based on firing probabilities of individual cells (the amount of produced traces was kept equal to the population model) to assess their repetition frequency discrimination performance (**Fig. 2c,d**).

A **Supplementary Methods Checklist** is available.

51. Grinvald, A., Lieke, E., Frostig, R.D., Gilbert, C.D. & Wiesel, T.N. Functional architecture of cortex revealed by optical imaging of intrinsic signals. *Nature* **324**, 361–364 (1986).

52. Aravanis, A.M. *et al.* An optical neural interface: *in vivo* control of rodent motor cortex with integrated fiberoptic and optogenetic technology. *J. Neural Eng.* **4**, S143–S156 (2007).
53. Guo, Z.V. *et al.* Flow of cortical activity underlying a tactile decision in mice. *Neuron* **81**, 179–194 (2014).
54. Miyashita, T., Shao, Y.R., Chung, J., Pourzia, O. & Feldman, D.E. Long-term channelrhodopsin-2 (ChR2) expression can induce abnormal axonal morphology and targeting in cerebral cortex. *Front. Neural Circuits* **7**, 8 (2013).
55. Cardin, J.A. *et al.* Targeted optogenetic stimulation and recording of neurons *in vivo* using cell type-specific expression of Channelrhodopsin-2. *Nat. Protoc.* **5**, 247–254 (2010).
56. Wichmann, F.A. & Hill, N.J. The psychometric function. I. Fitting, sampling, and goodness of fit. *Percept. Psychophys.* **63**, 1293–1313 (2001).
57. Trevelyan, A.J. & Jack, J. Detailed passive cable models of layer 2/3 pyramidal cells in rat visual cortex at different temperatures. *J. Physiol. (Lond.)* **539**, 623–636 (2002).